SURVEY PAPER

Subsonic aerofoil design 2010

D. M. Somers
dan@airfoils.com
Airfoils Inc
Pennsylvania, USA

ABSTRACT

The state of the art as practiced by a handful of aerofoil designers is discussed. The methods used, both theoretical and experimental, are described. Aerofoil/application design integration and expansion of the design envelope to lower and higher Reynolds numbers are illustrated by examples, including the slotted, natural-laminar-flow aerofoil.

NOMENCLATURE

Values are given in SI Units. Measurements and calculations were made in US Customary Units.

c	aerofoil chord, mm
c_c	section chord-force coefficient, $\oint C_p \, \mathrm{d}\left(\frac{z}{c}\right)$
c_d	section profile-drag coefficient, $\int_{\text{wake}} c_d' \mathrm{d}\left(\frac{h}{c}\right)$, except post stall, $c_n \sin\alpha + c_c \cos\alpha$
c_d'	point drag coefficient[1]
c_l	section lift coefficient, $c_n / \cos\alpha - c_d \tan\alpha$
c_m	section pitching-moment coefficient about quarter-chord point, $-\oint C_p \left(\frac{x}{c} - 0{\cdot}25\right) \mathrm{d}\left(\frac{x}{c}\right) + \oint C_p \left(\frac{z}{c}\right) \mathrm{d}\left(\frac{z}{c}\right)$
c_n	section normal-force coefficient, $-\oint C_p \, \mathrm{d}\left(\frac{x}{c}\right)$
C_L	aircraft lift coefficient
C_p	pressure coefficient, $\frac{p_l - p_\infty}{q_\infty}$
h	horizontal width in wake profile, mm
$(L/D)_{wing}$	wing lift-to-drag ratio
M	free-stream Mach number
n	amplification factor
N	critical amplification factor
p	static pressure, Pa
q	dynamic pressure, Pa
R	Reynolds number based on free-stream conditions and aerofoil chord
x	aerofoil abscissa, mm
z	aerofoil ordinate, mm
α	angle of attack relative to x-axis, deg
ν	arc limit in circle plane

Subscripts

cruise	cruise condition
l	local point on aerofoil
max	maximum
S	separation
T	transition
∞	free-stream conditions

Paper No. 3691. Manuscript received 3 November 2010, revised version received 20 December 2010, accepted 27 January 2010.
The latest in an occasional series of survey articles by leaders in their field focusing on a specific aspect of the aeronautical industry.

https://doi.org/10.1017/S0001924000005546 Published online by Cambridge University Press

Abbreviations

CFD	computational fluid dynamics
DLR	Deutsches Zentrum für Luft- und Raumfahrt e.V.
L.	lower surface
LFC	laminar flow control
LTPT	NASA Langley Low-Turbulence Pressure Tunnel
LSLTT	The Pennsylvania State University Low-Speed, Low-Turbulence Wind Tunnel
LSLTWT	Delft University of Technology Low-Speed Low-Turbulence Wind Tunnel
NACA	National Advisory Committee for Aeronautics
NASA	National Aeronautics and Space Administration
NLF	natural laminar flow
S.	boundary-layer separation location, x_s/c
SNLF	slotted, natural laminar flow
T.	boundary-layer transition location, x_T/c
U.	upper surface

1.0 HISTORICAL BACKGROUND

Aerofoil design has advanced considerably over the past century. The first aerofoil shapes were mere approximations of birds's wings. A random assortment of trial-and-error shapes, some of which were tested in simple low Reynolds number wind tunnels, followed. In the United States, the National Advisory Committee for Aeronautics (NACA) recognised the significance of aerofoils as a cornerstone of aeronautical research and development. In its first Annual Report to Congress, NACA called for '*the evolution of more efficient wing sections of practical form, embodying suitable dimensions for an economical structure, with moderate travel of the center of pressure and still affording a large range of angle of attack combined with efficient action*.'[2] By 1920, NACA had published a compendium of experimental results from various sources, most of them European[3]. Soon thereafter, NACA began the development of aerofoils at its Langley Memorial Aeronautical Laboratory[4]. Its first series of aerofoils, designated '*M sections*' after Max M. Munk, was tested at flight Reynolds numbers in the Langley Variable-Density Tunnel[5]. This series represents the first systematic approach to aerofoil development. The empirical design procedure, which involved perturbing the geometry of an existing shape, culminated in the development of the NACA four- and five-digit-series aerofoils in the 1930s[6–8].

Concurrently, Eastman N. Jacobs of NACA began work on laminar-flow aerofoils, having been inspired by discussions with B. Melvill Jones and G.I. Taylor in England. The design of an aerofoil that would exhibit a certain boundary-layer development and, correspondingly, the desired section characteristics required the inversion of the aerofoil analysis method of Theodore Theodorsen[9], also of NACA. Such an inverse method allows the aerofoil shape to be determined from a specified pressure distribution. At the time, however, little was known about the pressure distribution needed to promote laminar flow, only that the pressure should decrease with streamwise distance from the leading edge.

This procedure then represents the fundamental idea behind modern aerofoil design: the desired section characteristics result from the boundary-layer development which results from the pressure distribution which results from the aerofoil shape. The inverse method transforms the pressure distribution into the aerofoil geometry. The aerofoil designer must, however, intuitively or empirically deduce the pressure distribution that will produce the desired section characteristics.

The NACA 2- through 7-series aerofoils, the most famous of which are the 6-series, were evaluated in the Langley Low-Turbulence Tunnel and later the Langley Low-Turbulence Pressure Tunnel in the late 1930s and early 1940s[10,11]. The resulting catalog of systematically designed and experimentally validated aerofoils[11,12] was made available to all, and then NACA discontinued their low-speed aerofoil work, moving on to high-speed aerodynamics. The NACA four- and five-digit-series (turbulent-flow) aerofoils exhibited high maximum lift coefficients but also high profile-drag coefficients, whereas the 6-series (laminar-flow) aerofoils offered the possibility of low drag coefficients but the certainty of low maximum lift coefficients. The quandary faced by aircraft designers of the day was decided by the available construction techniques, which produced wing surfaces insufficiently smooth and rigid to sustain extensive laminar flow.

Meanwhile, in Germany, F.X. Wortmann and Richard Eppler began laminar-flow aerofoil design efforts at Universität Stuttgart. Wortmann used simple singularity and integral boundary-layer methods[13–15] to develop a catalog of aerofoils primarily for sailplanes[16]. Because the theoretical methods employed were crude, final evaluation of the aerofoils was done in a low-turbulence wind tunnel. Eppler, conversely, pursued the development of more precise theoretical methods[17,18].

The successor to NACA, the National Aeronautics and Space Administration (NASA), returned to aerofoil research in the 1960s with the design of the supercritical aerofoil by Richard T. Whitcomb[19]. The measured low-speed characteristics of the supercritical aerofoils were surprisingly good, leading to the design of a series of turbulent-flow aerofoils for low-speed aircraft[20], under the assumption that the construction techniques employed within general aviation were unsuitable for the achievement of laminar flow. Although the NASA turbulent-flow aerofoils did achieve high maximum lift coefficients, their cruise drag coefficients were no lower than those of the NACA turbulent-flow aerofoils. Accordingly, NASA's focus shifted to natural-laminar-flow (NLF) aerofoils, with the goal of combining the low-drag characteristics of the NACA 6-series aerofoils and the high-lift characteristics of the NASA low-speed aerofoils[21]. In this context, the term '*natural-laminar-flow aerofoil*' means an aerofoil capable of achieving significant extents of laminar flow ($\geq$ 30 per cent chord) on both the upper and lower surfaces simultaneously through favorable pressure gradients alone (i.e. without active boundary-layer control, such as suction or cooling).

The advent of composite structures[22] and increases in fuel costs drove the resurgence in NLF research. Such structures allow NLF aerofoils to achieve, in practice, the low drag coefficients measured in low-turbulence wind tunnels[23].

NASA, like its predecessor, NACA, has recently curtailed its aerofoil research efforts in favor of other activities. Much of the research has again shifted to Europe, in particular, DLR Braunschweig, Delft University of Technology, and Universität Stuttgart.

Today, aerofoils are being designed for an ever-widening range of applications[24], such as unmanned aerial vehicles[25], cooling-tower fans[26], sailplanes[27,28], wind turbines[29,30], rotorcraft[31], general aviation[32], including business jets[33], and regional[34] and transport aircraft[35].

2.0 THEORY VERSUS EXPERIMENT

It must be emphasised that NASA's goal was not the design of a series of NLF aerofoils but rather, as Richard Eppler had pioneered, the development of methods and their calibration to allow aerofoils to be designed for specific applications. The key to the success of this approach is the validation of the methods. The specific objective of the NASA effort then was code calibration via selective testing of a range of aerofoil concepts in the Langley Low-Turbulence Pressure Tunnel.

This approach was contrary to that taken by NACA and later F.X. Wortmann, who developed catalogs of aerofoils from which aircraft designers could choose shapes suitable to their applications. That approach was the only one available to NACA because the theoretical methods at that time were too primitive to accurately

https://doi.org/10.1017/S0001924000005546 Published online by Cambridge University Press

predict section characteristics. The use of catalogs has been successful, however, because the applications, aircraft having moderate Reynolds numbers, essentially incompressible Mach numbers, and low operational lift coefficients, were those for which the aerofoils had been designed. Also, the section characteristics were meticulously measured in low-turbulence wind tunnels *at the appropriate Reynolds numbers*. Thus, the aerofoil designs, their measured characteristics, and their applications coincided well.

As applications have become more diverse, however, the old aerofoils and their measured characteristics have become less suitable. Today, with applications ranging from high-altitude propellers to large tiltrotors, the use of aerofoils developed for propeller-driven low-speed aircraft is unacceptable. Indeed, for many of today's applications, the use of such aerofoils is unwise because the design requirements for the old low-speed aircraft aerofoils are vastly different from those for the intended applications; stall-regulated wind turbines are a prime example[29].

Catalogs exhibit inadequate coverage as well. Each application requires a particular performance from the aerofoil. Even if this performance falls within the range of characteristics covered by a catalog, it is unlikely an aerofoil from the catalog will match exactly the requirements of the application.

Another advantage of theoretical aerofoil design methods is the ability to economically explore many concepts. Such efforts are usually impractical experimentally because of the associated time and cost.

Thus, the need for a theoretical aerofoil design method is threefold: for the design of aerofoils that fall outside the range of applicability of available catalogs, for the design of aerofoils that exactly match the requirements of the application, and for the economic exploration of various aerofoil concepts.

Finally, one further obstacle, summarised by the following saying, must be overcome:

No one believes the theory except the one who developed it.
Everyone believes the experiment except the one who ran it.

This saying again emphasises the requirement for rigorous validations of the methods.

2.1 Theories

Three theoretical methods have become widely employed around the world: the Eppler Airfoil Design and Analysis Code (PROFIL)[24,36] and the XFOIL[37] and MSES[38] codes. The PROFIL and XFOIL codes incorporate compressibility corrections, which restrict their use to locally subcritical flows, whereas the MSES code, which incorporates an Euler solver, is capable of handling transonic flows. A comparison of the inviscid pressure distributions for a 12-percent-thick symmetric aerofoil at a Mach number of 0·74 predicted by the PROFIL and MSES codes is shown in Fig. 1.

The Eppler code contains a conformal-mapping method for the design of aerofoils with prescribed velocity-distribution characteristics, a higher-order panel method for the analysis of the potential flow about given aerofoils, and an integral boundary-layer method. Thus, aerofoils with prescribed boundary-layer characteristics can be designed and aerofoils with prescribed shapes can be analysed.

In all other inverse methods, the velocity (or pressure) distribution is specified at one angle of attack and the aerofoil shape that will exhibit that velocity distribution is computed. Thus, the aerofoil is designed at a single point. All other conditions are considered off-design and must be taken into account intuitively and analysed later to determine acceptability.

The conformal-mapping method in the Eppler code is unique because it allows the velocity distribution to be specified along different segments of the aerofoil at different angles of attack. This is an extremely powerful capability because it allows the important features of many velocity distributions to be incorporated into the aerofoil design from the outset. Thus, the aerofoil is designed at several points simultaneously and the off-design conditions can be taken into account in the initial specification.

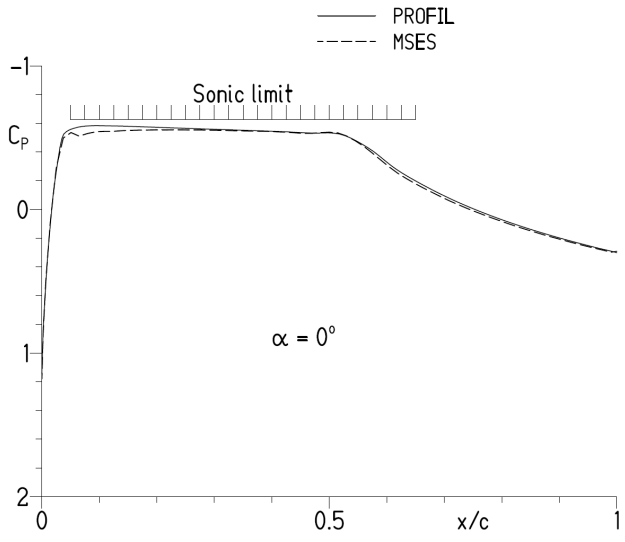


Figure 1. Comparison of inviscid pressure distributions for symmetric aerofoil at α = 0° and M = 0·74.

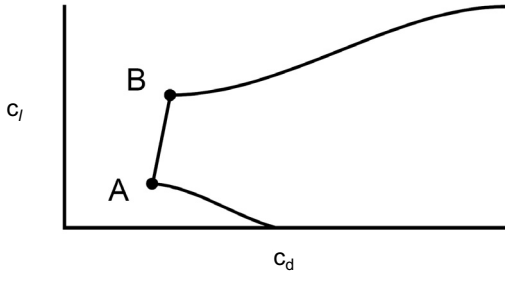


Figure 2. Sketch of aerofoil drag polar.

Figure 2 helps to illustrate, in a very simplified way, the use of this capability. As determined from the desired application performance, the aerofoil should exhibit low profile-drag coefficients over the range of lift coefficients from points A to B. Point A corresponds to the lift coefficient below which transition moves rapidly forward along the lower surface. Thus, for this point, the design of the lower surface is critical. Point B corresponds to the lift coefficient above which transition moves rapidly forward on the upper surface. For this point, the upper surface is critical. Using other design methods, the velocity distribution must be specified at point A or point B or possibly an intermediate point. Using the Eppler code, the velocity distribution along the lower surface at point A is specified as is the distribution along the upper surface at point B, thus simultaneously satisfying the requirements at both points.

An integral method is used for the prediction of the boundary-layer development for each velocity distribution. The method can predict laminar and turbulent boundary layers, including separation. Transition is predicted by a full, as opposed to an envelope, e^N method[39,40]. The effect of laminar separation bubbles on the profile-drag coefficients is also computed.

A key feature of the Eppler code is the connection between the boundary-layer and conformal-mapping methods. This connection allows the boundary-layer characteristics to be controlled directly during the aerofoil design process. This is a particularly important capability for the design of laminar-flow aerofoils and represents a major advancement over the procedure used for the design of the

https://doi.org/10.1017/S0001924000005546 Published online by Cambridge University Press

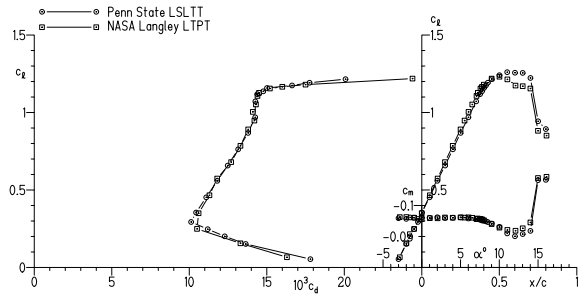


Figure 3. Comparison of experimental section characteristics of E 387 aerofoil for R = 200,000 with transition free.

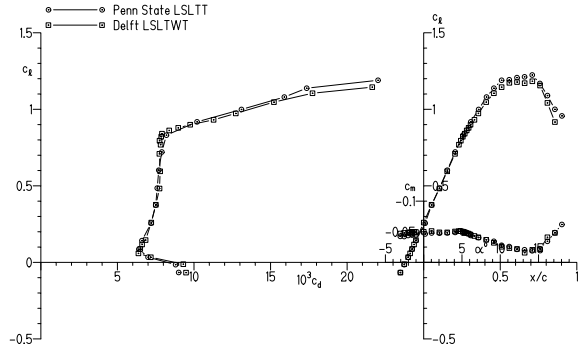


Figure 4. Comparison of experimental section characteristics of S805 aerofoil for R = 1 × 10^6 with transition free.

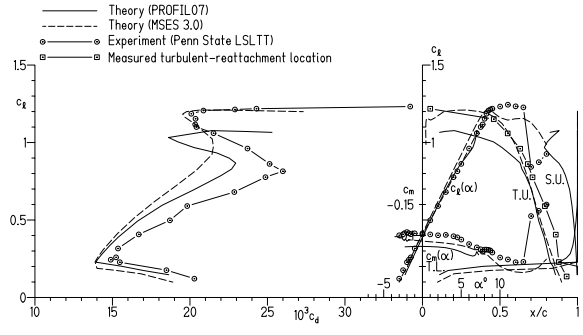


Figure 5. Comparison of theoretical and experimental section characteristics of E 387 aerofoil for R = 100,000 with transition free.

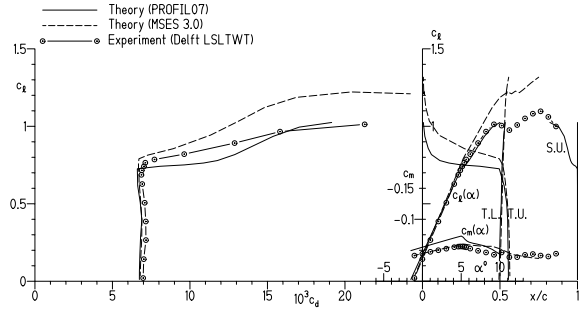


Figure 6. Comparison of theoretical and experimental section characteristics of S809 aerofoil for R = 2 × 10^6 with transition free.

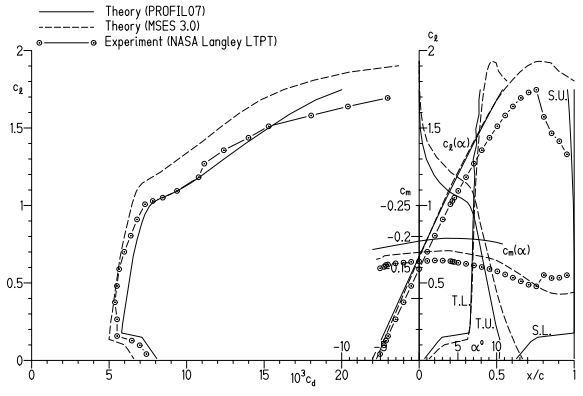


Figure 7. Comparison of theoretical and experimental section characteristics of S825 aerofoil for R = 6 × 10^6 with transition free.

NACA laminar-flow aerofoils. Now, instead of intuitively or empirically deducing the velocity distribution that will exhibit the desired boundary-layer characteristics, the designer can determine directly the modifications to the velocity distribution required to produce the desired boundary-layer development at any given angle of attack[24].

2.2 Experiments

It is paramount that aerofoils be evaluated in wind tunnels having excellent flow quality. The use of wind tunnels having higher turbulence levels (> ~0·1 percent) produces inaccurate results, which cannot be corrected, especially for aerofoils capable of exhibiting extensive laminar flow. The most obvious effects are to increase the profile-drag coefficient for high Reynolds numbers and to decrease the drag coefficient for low Reynolds numbers. Neither effect is '*conservative*.' In the former case, a good aerofoil may be rejected and, in the latter, overly optimistic performance is awaited, based on the wind-tunnel results, but not realised on the application.

At present, only two thoroughly validated facilities for two-dimensional testing exist: the Delft University of Technology Low-Speed Low-Turbulence Wind Tunnel (LSLTWT)[41] in The Netherlands and The Pennsylvania State University Low-Speed, Low-Turbulence Wind Tunnel (LSLTT)[42] in the United States. Regrettably, the NASA Langley Low-Turbulence Pressure Tunnel (LTPT)[43,44], which is the only facility in the world capable of low-speed laminar-flow aerofoil testing at high Reynolds numbers (> 6 × 10^6), has recently been shut down. This is a major loss for verification of aerofoils operating at high Reynolds numbers and for code validation.

Both the Penn State LSLTT and the Delft LSLTWT are closed-throat single-return atmospheric tunnels. The test section of the Penn State tunnel is 101cm high by 148cm wide, whereas that of the Delft tunnel is 125cm high by 180cm wide. In both tunnels, electrically actuated turntables provide positioning and attachment for the two-dimensional models, the turntables are flush with the top and bottom tunnel walls and rotate with the models, which are mounted vertically between the turntables, and the gaps between the models and the turntables are sealed. The turbulence intensity in the test section of the Penn State tunnel is approximately 0·05 per cent at 46ms^{-1}, whereas the turbulence level in the test section of the Delft tunnel varies from 0·02 per cent at 10ms^{-1} to 0·04 per cent at 60ms^{-1} to 0·10 per cent at 85ms^{-1}.

Because all the experimental results and most of the theoretical results presented were obtained at Mach numbers less than 0·2 (i.e. incompressible), the Mach number is shown only if it is greater than 0·2. A comparison of the section characteristics of the 9-per-cent-thick E 387 aerofoil[45] for a Reynolds number of 200,000 from the Penn State LSLTT[46] and the NASA Langley LTPT[47] is shown in Fig. 3.

https://doi.org/10.1017/S0001924000005546 Published online by Cambridge University Press

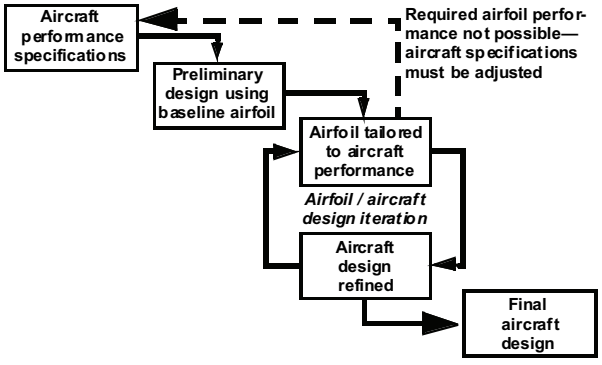


Figure 8. Aerofoil/aircraft design integration.

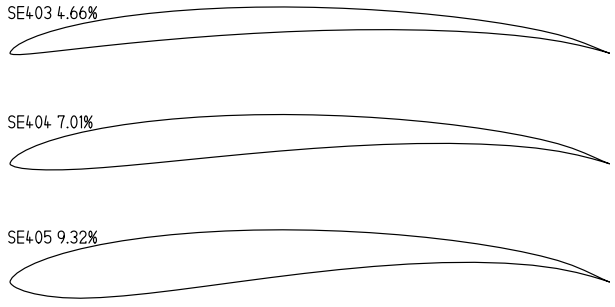


Figure 9. SE403, SE404, and SE405 aerofoil shapes.

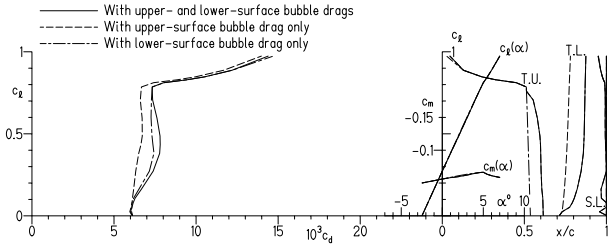


Figure 10. Theoretical section characteristics of S805 aerofoil for R = 1 × 10^6.

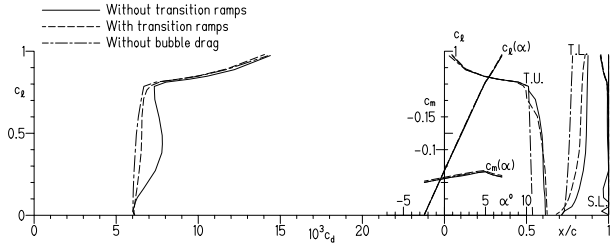


Figure 11. Theoretical section characteristics of S805 aerofoil for R = 1 × 10^6 with and without transition ramps.

A comparison of the section characteristics of the 13·5-per-cent-thick S805 aerofoil[48] for a Reynolds number of 1 × 10^6 from the Penn State[49] and Delft[48] tunnels is shown in Fig. 4. The agreement is considered excellent.

Theoretical and experimental results for the E 387 aerofoil[46] are compared in Fig. 5; for the 21-per-cent-thick S809 aerofoil[50], in Fig. 6; and, for the 17-per-cent-thick S825 aerofoil[51], in Fig. 7. These figures include, in addition to the usual section characteristics, the transition and separation locations. The agreement is typical and considered very good.

3.0 TAILORING TO SPECIFIC APPLICATIONS

3.1 Aerofoil/application design integration

A too-oft-heard proclamation is: '*Aerofoil XYZ is the best*.' For what? Aerofoils must be designed for applications. The process of integrating the aerofoil and application designs is illustrated in Fig. 8, using an aircraft as the application. The preliminary design does not require an actual baseline aerofoil. Particularly in the case of a novel application, realistic section characteristics, not a wish list, can be substituted. Correspondingly, the aircraft specifications must be adjusted should the required aerofoil performance prove impossible. The central aerofoil/aircraft design iteration emphasises the crucial cooperation that must occur between the aircraft and aerofoil designers. A successful outcome is predicated on a well-defined set of aerofoil design specifications, including all the operational conditions, again underlining the required cooperation between the designers. Note that the goal is not to design the best *aerofoil* but rather the best *aircraft*.

The same procedure can be used to modify an existing aircraft design, necessitated by weight growth, for example. The redesign is facilitated if this procedure was employed to design the original aerofoil.

3.2 Expanding the aerofoil design envelope

Given the current theoretical and experimental capabilities, it can be concluded that the design of aerofoils for moderate lift coefficients and Reynolds numbers has become straightforward. The challenge is to produce the highest performance for a specific application. At this point, the most productive area is probably the integration of structural and aerodynamic designs – always an area of conflict. Such a cooperation will likely lead to significant improvements in not only aircraft, especially rotorcraft, but also applications like wind turbines.

Even more challenging is the expansion of the aerofoil design envelope to lower and higher Reynolds numbers. Recently, a family of aerofoils (Fig. 9) was designed for a propeller intended to operate at an altitude of 30,000 metres. The planform and aerofoil designs were tightly integrated, producing a well-defined set of design specifications for the aerofoil family. Fortunately, the planned use of advanced composites and the light structural loads permitted the small aerofoil thicknesses mandated by the low Reynolds numbers. The aerofoils are completely laminar at the operating Reynolds number of 10,000.

The experimental verification of aerofoils for such extremely low Reynolds numbers will be difficult. Conventional test techniques involving pressure measurements on the model and in the wake are impractical because of the miniscule dynamic pressures. A promising technique is particle image velocimetry.

For more moderate Reynolds numbers (50,000 to 3 × 10^6), laminar separation bubbles are a major concern. The Eppler code contains two options that are particularly useful for alleviating drag-producing laminar separation bubbles. Note that not all laminar separation bubbles are detrimental. In many cases, bubbles provide an efficient mechanism for forcing transition. Accordingly, the promotion of '*benign*' laminar separation bubbles is often a goal. To that end, it is necessary first to know how much drag the bubbles are contributing. By disregarding the drag contribution on one surface, the contribution on the other surface can be determined, as shown in Fig. 10. Here the difference between the drag polar including the bubble drags on both surfaces (solid line) and the polar including the

https://doi.org/10.1017/S0001924000005546 Published online by Cambridge University Press

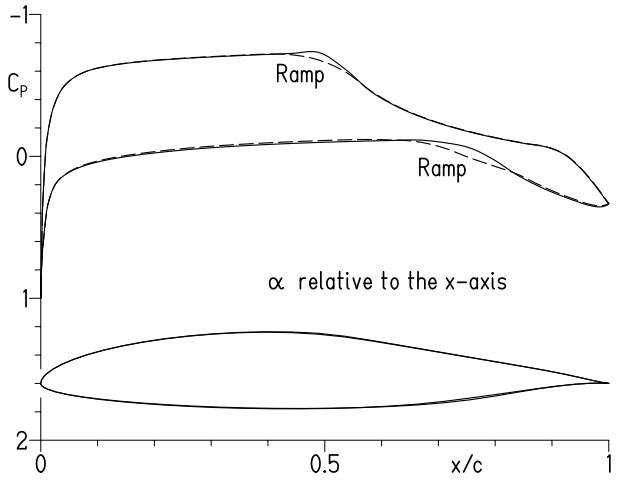


Figure 12. Inviscid pressure distribution for S805 aerofoil at c_l = 0·4 with and without transition ramps.

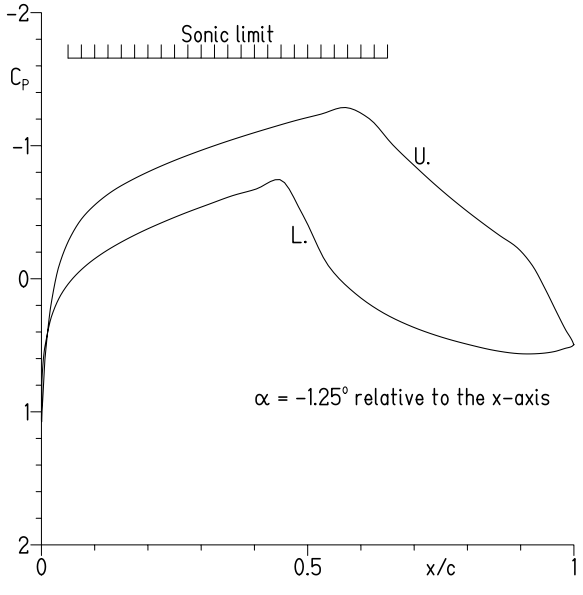


Figure 13. Inviscid pressure distribution for tiltrotor wing aerofoil at c_l = 0·6 and M = 0·55.

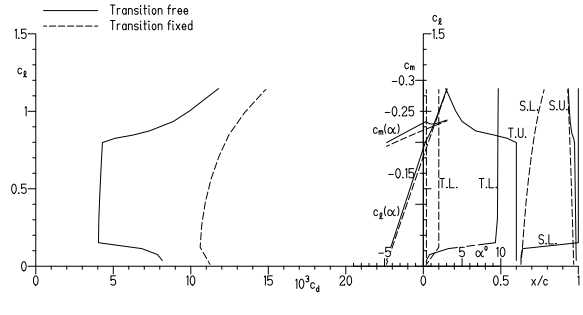


Figure 14. Theoretical section characteristics of tiltrotor wing aerofoil at M = 0·55 and R = 25 × 10^6 with transition free.

bubble drag on the upper surface only (dashed line) is the bubble drag on the lower surface. For the S805 aerofoil[48], the bubble drag on the lower surface is much larger than that on the upper surface. This capability allows transition ramps[52] to be developed precisely for each surface. The Eppler code includes an option that semi-automatically defines a curved transition ramp[53]; only the lengths of the ramp forward and aft of the beginning of the pressure recovery must be specified. The effect of such ramps on the drag polar is shown in Fig. 11. Note that, although the bubble drag is greatly reduced, it is not completely eliminated. The effects of the ramps on the pressure distribution and the aerofoil shape are illustrated in Fig. 12. This capability can also be used to position turbulators and evaluate their effect[27,54,55].

The S805 aerofoil and its modification to alleviate significant laminar separation bubbles is an example of beneficial interplay between theory and experiment. In 1984, when the S805 aerofoil was designed, the Eppler code only issued a warning if additional drag was to be expected from a laminar separation bubble; the amount of additional drag was not computed because the method did not model the effect of the bubble on the boundary-layer development downstream. The S805 aerofoil was designed such that the warning was just suppressed at the design Reynolds number of 1 × 10^6. The experiment showed significant bubble drag, which could be alleviated by turbulators. These results led to a sharper criterion for the warning and eventually to a sophisticated laminar separation bubble model. Interestingly, the bubble model required a more precise prediction of the transition location, which led to the replacement of the original two-parameter method with the e^N method.

The design of natural-laminar-flow aerofoils for higher Reynolds numbers (> 15 × 10^6) continues to receive attention. Because the reduction in skin friction due to laminar flow becomes larger with increasing Reynolds number, the achievement of extensive laminar flow at high Reynolds numbers can be an enabling technology for many applications, such as large tiltrotors. An example of a pressure distribution for such a design is shown in Fig. 13. The predicted section characteristics at a Mach number of 0·55 and a Reynolds number of 25 × 10^6 are shown in Fig. 14. The greater aerofoil performance due to laminar flow increases the lift-to-drag ratio of the wing (only) by about 60 percent at the operational lift coefficients, 0·55 to 0·60 (Fig. 15).

The lower-surface pressure distribution for the same tiltrotor wing aerofoil at one of the conditions for the lower limit of the low-drag, lift-coefficient range is shown in Fig. 16. This example incorporates the '*cow-belly*' concept originally proposed by Richard Eppler[56]. Just aft of the leading edge, the pressure gradient is strongly adverse and the flow just avoids laminar separation. Shortly thereafter, the pressure gradient becomes neutral and then strongly favorable until transition finally occurs at the beginning of the pressure recovery. Thus, the laminar boundary layer is pushed to the limit along its entire length and is therefore near transition everywhere. Such a pressure distribution represents a certain optimum. It allows extensive laminar flow at high Reynolds numbers, exhibits more camber at a given lift coefficient, therefore achieving a higher maximum lift coefficient, and shifts the loading forward, thus minimising the pitching-moment coefficient. The corresponding amplification-factor growth predicted by the full e^N transition-prediction method in the Eppler code is shown in Fig. 17. Here the amplification factor increases rapidly at first and then increasingly slowly downstream. An investigation of such distributions by Eppler indicates this is indeed optimal. Contrast this with the simple NACA 6-series pressure distribution, which becomes completely flat at a given angle of attack. The 6-series aerofoils exhibit pressure distributions within the low-drag range that are wastefully favorable forward and insufficiently favorable aft, which causes the laminar bucket to '*fill in*' with increasing Reynolds number[11]. Experimentally verifying such laminar-flow aerofoils at high Reynolds numbers is a problem because of the lack of suitable wind tunnels.

https://doi.org/10.1017/S0001924000005546 Published online by Cambridge University Press

The effect of leading-edge roughness on the section characteristics of NLF aerofoils represents another challenge. Of particular importance is the loss of maximum lift coefficient due to roughness. For many applications, such losses must be minimised. An example application is wind turbines, where the peak power of the turbine is directly proportional to the maximum lift coefficient, unlike most aircraft applications, where the stall speed is proportional to the square root of the lift coefficient.

A persistent myth, traceable to the NACA 6-series aerofoils[11], is that the maximum lift coefficient increases with increasing thickness. To study the effect of roughness as a function of aerofoil thickness and maximum lift coefficient, an experimental investigation of three related aerofoils was conducted[57]. Two aerofoils had the same thickness and two, the same predicted maximum lift coefficient, with one aerofoil common to both pairs. The three aerofoils form a minimal matrix allowing the evaluation of the effects of both aerofoil thickness and maximum lift coefficient on the sensitivity to roughness. The key to a valid comparison is the control of the transition location, which has a major influence on the maximum lift coefficient. The Eppler code was used to design the leading edges of the three aerofoils such that they would all exhibit the same transition movement around the maximum lift coefficient. The three aerofoil shapes are shown in Fig. 18 and the predicted transition location as a function of lift coefficient is shown in Fig. 19. (The lift coefficients of the S903 aerofoil have been shifted upward to account for its lower maximum lift coefficient.) Interestingly, the investigation showed that the effect of roughness increased with increasing aerofoil thickness, as had been commonly believed, but decreased slightly with increasing maximum lift coefficient, contrary to popular belief. More interestingly, the effect of roughness was independent of both aerofoil thickness and maximum lift coefficient if transition was merely fixed by trip strips near the leading edge; only a much more severe roughness, equivalent to NACA standard roughness[11], showed the effects.

3.3 Slotted, natural-laminar-flow aerofoil

Finally, the aerofoil/aircraft design integration can be guided by the appropriate use of figures of merit[58]. The figure of merit for reducing the profile drag of the wing, often the major contributor to the total aircraft drag in cruise, is $c_{l,max}/c_{d,cruise}$. Note the figure of merit is expressed in terms of section (i.e. aerofoil) characteristics, not aircraft characteristics. The figure of merit can be interpreted as follows. The wing area, and therefore the aircraft wetted area, can be reduced if a higher maximum lift coefficient is achieved, for a given minimum speed, resulting in lower drag. The wing profile drag can also be reduced if a lower section profile-drag coefficient is achieved. This figure of merit applies to almost all aircraft. For those aircraft having their wing area determined by a fuel-volume requirement (e.g. business jets), reducing the section profile-drag coefficient is even more beneficial.

Three approaches have become accepted for the reduction of wing profile drag. One approach is to employ a high-lift system (e.g. leading-edge slat plus double- or triple-slotted Fowler flap) to achieve a higher maximum lift coefficient[59]. This approach has several disadvantages. Almost no laminar flow can be achieved because of the disturbances introduced by the slat, which results in a high section profile-drag coefficient. The maximum lift coefficient is limited to about four, which limits the reduction in wing area. Such systems are complex, both mechanically and structurally, resulting in higher weight and cost. This approach can provide a wing profile-drag reduction of about 50 per cent compared to a conventional, turbulent-flow wing with no high-lift system. The drag reduction is due entirely to the high maximum lift coefficient. This approach has been adopted for all current transport aircraft. Active high-lift systems (e.g. blown flaps and circulation control) have demonstrated very high maximum lift coefficients, but the cost, complexity, and potentially disastrous failure modes have prevented their adoption in production civil aircraft.

A second approach is to employ a natural-laminar-flow (NLF) aerofoil to achieve a lower profile-drag coefficient[10]. By appropriate aerofoil shaping, extensive laminar flow can be achieved on both the upper and lower wing surfaces. The extent of laminar flow is limited by the pressure-recovery gradient on the upper surface. The recovery gradient becomes steeper as the extent of the favorable pressure gradient increases, eventually reaching a limit beyond which trailing-edge separation occurs, resulting in a lower maximum lift coefficient and, correspondingly, a lower figure of merit. (Leading-edge sweep also affects the extent of laminar flow because it introduces crossflow instabilities that lead to transition.) This approach can provide a wing profile-drag reduction of about 50 per cent compared to a conventional, turbulent-flow wing. It does, however, require more stringent construction techniques and maintenance. The drag reduction is due entirely to the low profile-drag coefficient. This approach has been adopted for most current general-aviation aircraft, including business jets, as well as unmanned aerial vehicles and all sailplanes.

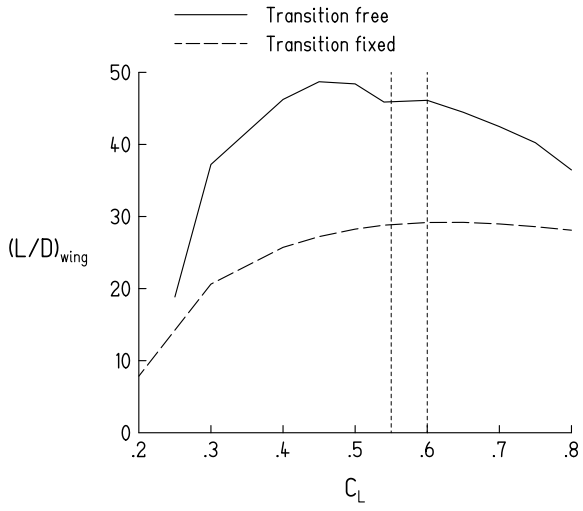


Figure 15. Theoretical lift-to-drag ratio of tiltrotor wing at M = 0·55 and R = 25 × 10^6.

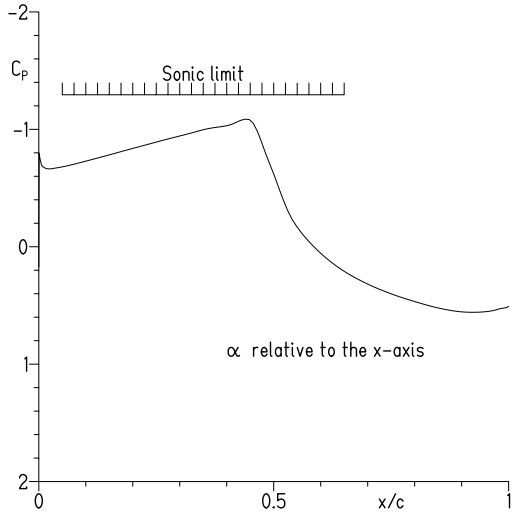


Figure 16. Inviscid lower-surface pressure distribution for tiltrotor wing aerofoil at α = −4° and M = 0·60.

https://doi.org/10.1017/S0001924000005546 Published online by Cambridge University Press

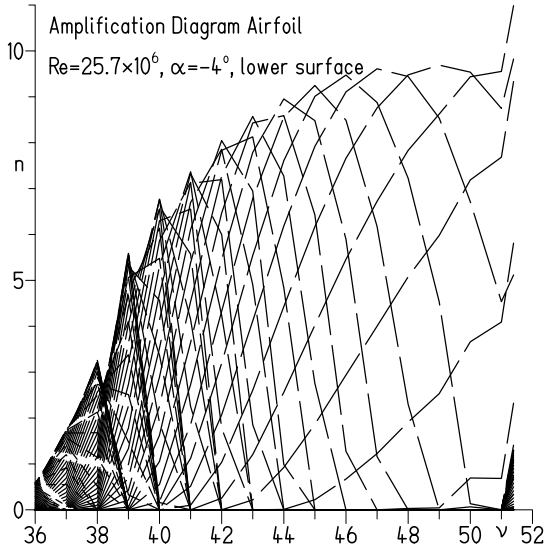


Figure 17. Theoretical amplification-factor growth for tiltrotor wing aerofoil at M = 0·60.

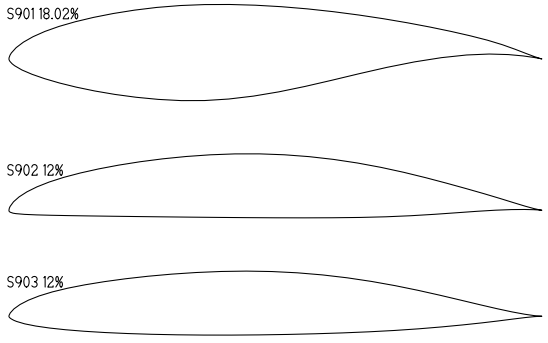


Figure 18. S901, S902, and S903 aerofoil shapes.

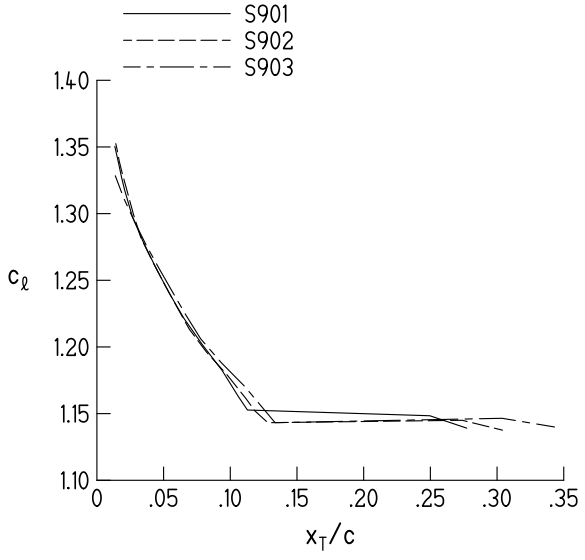


Figure 19. Variation of theoretical transition location with lift coefficient for S901, S902, and S903 aerofoils for R = 1 × 10^6.

A third approach is to employ a laminar-flow-control (LFC) aerofoil to achieve a lower profile-drag coefficient[60]. By incorporating suction through porous or slotted wing skins, 100-per-cent-chord laminar flow can be achieved on both the upper and lower surfaces. LFC systems are very complex, mechanically, structurally, and operationally, resulting in higher weight and cost. This approach can provide a wing profile-drag reduction of about 75 per cent compared to a conventional, turbulent-flow wing. The drag reduction is due entirely to the low profile-drag coefficient. This approach has yet to be adopted for any production aircraft, although leading-edge suction is being explored to alleviate crossflow instabilities on the tail of the next version of the Boeing 787 aircraft.

A new approach, called the slotted, natural-laminar-flow (SNLF) aerofoil[61], has been developed. The SNLF aerofoil concept is similar in nature to the slotted, supercritical aerofoil concept[19]. in that it employs a slot to allow a pressure recovery that would not be possible for a single-element aerofoil.

The pressure distribution for the 14-per-cent-thick S414 SNLF aerofoil[62] is shown in Fig. 20. Unlike all the other aerofoils, which were designed using only the Eppler code, the S414 aerofoil was designed using the Eppler and MSES codes. At this angle of attack, the fore-element loading is low. As the angle of attack increases, the aft-element loading is essentially constant, whereas the fore-element loading increases – not unlike an aft-loaded single-element aerofoil.

Because the aft element eliminates the requirement that the pressure at the trailing edge of the fore element recover to free stream, the favorable pressure gradient can extend further aft. For the SNLF aerofoil concept, the favorable gradient extends along both surfaces of the fore element to near its trailing edge. Thus, the fore element is entirely laminar. (Because of the concave curvature of the fore-element lower surface in the slot, the laminar boundary-layer there may be impacted by Görtler instabilities[63] for Reynolds numbers greater than about 3 × 10^6.) The aft element then provides the necessary recovery to free-stream pressure. Because the wake of the fore element does not impinge on the aft element, the aft element can also achieve significant extents of laminar flow. On the aft element of the S414 aerofoil, laminar flow extends to about 60-per-cent chord on the upper surface and to the trailing edge on the lower surface.

The SNLF aerofoil concept allows the extent of laminar flow to be increased beyond the limit for (single-element) NLF aerofoils previously mentioned. Thus, the concept allows low profile-drag coefficients to be achieved without having to resort to the complexity and cost of LFC and high maximum lift coefficients to be achieved without variable geometry (Fig. 21)[62]. Accordingly, the wing drag reduction is due to both the high maximum lift coefficient and the low profile-drag coefficient.

The SNLF aerofoil shape is not radically different from conventional aerofoil shapes – no more than conventional, NLF aerofoils are from conventional, turbulent-flow aerofoils. Unlike conventional aerofoils with slotted flaps, however, the SNLF aerofoil has no nested configuration; the slot between the fore and aft elements is always open.

4.0 ART VERSUS SCIENCE

While portions of the aerofoil design process now clearly fall within the realm of science, other portions are best described as art. The connection between the desired boundary-layer development and the corresponding pressure distribution is still tenuous. Indeed, the reliable prediction of the dominant phenomenon of turbulent separation is still elusive. The incorporation of a full e^N transition-prediction method into both the Eppler and MSES codes has greatly improved the predictions of not only the profile-drag coefficient within the low-drag range but the limits of the low-drag range as well. At this juncture, it is probably not too brave to state that the prediction of section characteristics within the linear lift-curve range

https://doi.org/10.1017/S0001924000005546 Published online by Cambridge University Press

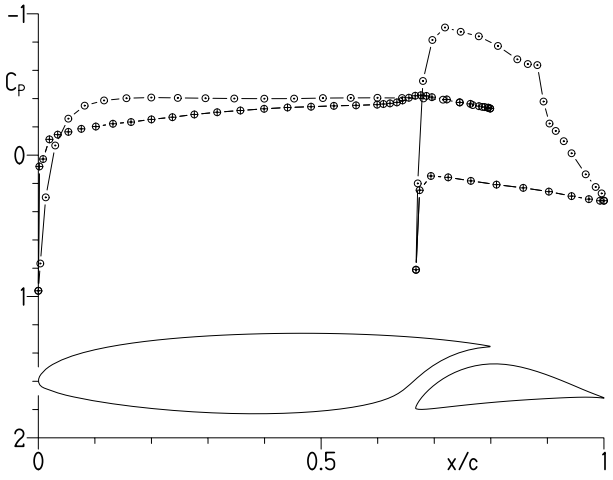


Figure 20. Experimental pressure distribution for S414 aerofoil at c_l = 0·3 for R = 1 × 10^6 with transition free. Open symbols represent data for upper surface; crossed symbols, data for lower surface.

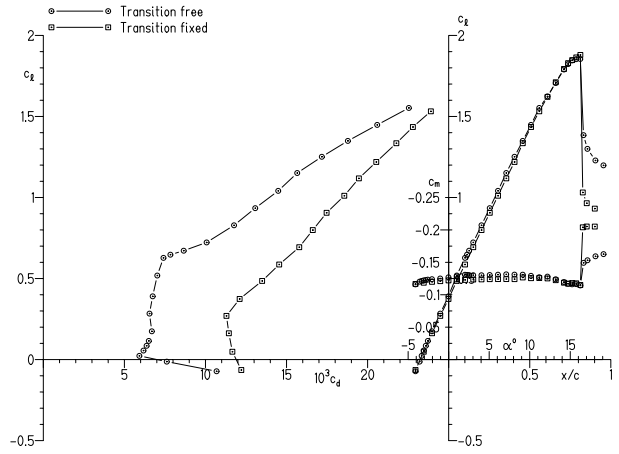


Figure 21. Experimental section characteristics of S414 aerofoil for R = 1 × 10^6.

is accurate enough for most applications. The prediction of laminar separation, the resulting bubbles, and their effect on the section characteristics is also quite precise.

The prediction of turbulent separation and its effect on section characteristics, primarily the maximum lift coefficient, is another matter. As a colleague recently ventured, if the methods could predict the maximum lift coefficient, there would be little need for further low-speed aerofoil testing – except to validate the methods, not an insignificant task. The most recent computational fluid dynamics (CFD) codes cannot predict the two-dimensional maximum lift coefficient any more accurately than the traditional methods[64]. This then remains the most significant challenge for method development.

Related deficiencies are the prediction and measurement of the effect of massive separation on the section characteristics. These post-stall characteristics play important roles for many applications. Add to that the vagaries of dynamic stall and the future work available is staggering.

5.0 CONCLUDING REMARKS

I am often told my aerofoils look like Eppler or Wortmann or … aerofoils, to which I respond, '*You are right. All aerofoils are the same – they are all round in the front and sharp in the back.*' To the unenlightened, all aerofoils do look alike, but, as the saying goes, God is in the details.

ACKNOWLEDGMENTS

I am grateful to NASA Langley Research Center, the National Renewable Energy Laboratory (NREL), the US Army, and others for supporting my, at times controversial, efforts.

REFERENCES

1. PANKHURST, R.C. and HOLDER, D.W. *Wind-Tunnel Technique*, Sir Isaac Pitman & Sons, London, UK, 1965.
2. National Advisory Committee for Aeronautics. First Annual Report of the National Advisory Committee for Aeronautics, 1915.
3. National Advisory Committee for Aeronautics. Aerodynamic characteristics of aerofoils, NACA Rep 93, 1920.
4. HANSEN, J.R. *Engineer in charge*, NASA SP-4305, 1987.
5. MUNK, M.M. and MILLER, E.W. Model tests with a systematic series of 27 wing sections at full Reynolds number, NACA Rep 221, 1925.
6. JACOBS, E.N., WARD, K.E. and PINKERTON, R.M. The characteristics of 78 related airfoil sections from tests in the variable-density wind tunnel, NACA Rep 460, 1933.
7. JACOBS, E.N., PINKERTON, R.M. and GREENBERG, H. Tests of related airfoils having the maximum camber unusually far forward, NACA Rep 537, 1935.
8. JACOBS, E.N., PINKERTON, R.M. and GREENBERG, H. Tests of related forward-camber airfoils in the variable-density wind tunnel, NACA Rep 610, 1937.
9. THEODORSEN, T. Theory of wing sections of arbitrary shape, NACA Rep 411, 1932.
10. JACOBS, E.N. Preliminary report on laminar-flow airfoils and new methods adopted for airfoil and boundary-layer investigations, NACA WR L-345, 1939 (formerly, NACA ACR).
11. ABBOTT, I.H., VON DOENHOFF, A.E. and STIVERS, L.S., JR Summary of Airfoil Data, NACA Rep 824, 1945. (Supersedes NACA WR L-560.)
12. ABBOTT, I.H. and VON DOENHOFF, A.E. *Theory of Wing Sections*, Dover Publications, New York, USA, 1959.
13. TRUCKENBRODT, E. Die Berechnung der Profilform bei vorgegebener Geschwindigkeitsverteilung (The Calculation of the Profile Shape from Specified Velocity Distribution), *Ingenieur-Archiv*, 1951, **19**, (6), pp 365–377.
14. TRUCKENBRODT, E. A method of quadrature for calculation of the laminar and turbulent boundary layer in case of plane and rotationally symmetrical flow, NACA TM 1379, 1956. (Translated from *Ingenieur-Archiv*, 1952, **20**, (4), pp 211–228.)
15. WORTMANN, F.X. Progress in the design of low-drag aerofoils, in*: Boundary Layer and Flow Contro*l, **2**, LACHMANN, G.V. (Ed), Pergamon Press, London, UK, 1961, pp 748–770.
16. ALTHAUS, D. and WORTMANN, F.X. *Stuttgarter Profilkatalog I (Stuttgart Profile Catalog I)*, Friedr. Vieweg & Sohn, Braunschweig, Germany, 1981.
17. EPPLER, R. Direct calculation of airfoils from pressure distribution, NASA TT F-15,417, 1974. (Translated from *Ingenieur-Archiv*, 1957, **25**, (1), pp 32–57.)
18. EPPLER, R. Practical calculation of laminar and turbulent bled-off boundary layers, NASA TM-75328, 1978. (Translated from *Ingenieur-Archiv*, 1963, **32**, (4), pp 221–245.)
19. WHITCOMB, R.T. and CLARK, L.R. An airfoil shape for efficient flight at supercritical Mach numbers, NASA TM X-1109, 1965.
20. MCGHEE, R.J., BEASLEY, W.D. and WHITCOMB, R.T. NASA low- and medium-speed airfoil development, NASA TM-78709, 1979.
21. SOMERS, D.M. Subsonic Natural-Laminar-Flow Airfoils, in: *natural laminar flow and laminar flow control,* BARNWELL, R.W. and HUSSAINI, M.Y. (Eds), Springer-Verlag New York, USA, 1992, pp 143–176.

https://doi.org/10.1017/S0001924000005546 Published online by Cambridge University Press

22. NAEGELE, H. and EPPLER, R. Plastic sailplane FS-24 Phoenix, *Soaring*, July-August 1958, **22**, (4), pp 2–5. (Translated from *Aero Revue*, March 1958, **33**, pp 140–143.)
23. EPPLER, R. Some new airfoils, in: Science and Technology of Low Speed and Motorless Flight, NASA CP-2085, Part I, 1979, pp 131–153.
24. EPPLER, R. *Airfoil Design and Data*, Springer-Verlag Berlin, Germany, 1990.
25. MAUGHMER, M.D. and SOMERS, D.M. Design and experimental results for a high-altitude, long-endurance airfoil, *J Aircr*, February 1989, **26**, (2), pp 148–153.
26. SOMERS, D.M. The S904 and S905 airfoils, NREL/SR-500-36338, 2005.
27. HORSTMANN, K.H., QUAST, A. and BOERMANS, L.M.M. Pneumatic turbulators – a device for drag reduction at Reynolds numbers below 5 * 10^6, AGARD-CP-365, 1984, pp 20-1–20-19.
28. BOERMANS, L.M.M. and VAN GARREL, A. Design and windtunnel test results of a flapped laminar flow airfoil for high-performance sailplane applications, ICAS-94-5.4.3, Anaheim, USA, September 1994.
29. TANGLER, J.L. and SOMERS, D.M. NREL airfoil families for HAWTs, NREL/TP-442-7109, 1995.
30. TIMMER, W.A. and VAN ROOIJ, R.P.J.O.M. Summary of the Delft University wind turbine dedicated airfoils, AIAA Paper 2003-0352, January 2003.
31. SOMERS, D.M. Some new airfoils for rotorcraft, US Army RDECOM TR 10-D-71, 2010. (Available from DTIC.)
32. SELIG, M.S., MAUGHMER, M.D. and SOMERS, D.M. Natural-laminar-flow airfoil for general-aviation applications, *J Aircr*, July-August 1995, **32**, (4), pp 710–715.
33. FUJINO, M., YOSHIZAKI, Y. and KAWAMURA, Y. Natural-laminar-flow airfoil development for a lightweight business jet, *J Aircr*, July-August 2003, **40**, (4), pp 609–615.
34. SOMERS, D.M. and HORSTMANN, K.-H. Design of a medium-speed, natural-laminar-flow airfoil for commuter aircraft application, DFVLR IB 129-85/26, 1985.
35. KÖRNER, H., HORSTMANN, K.H., KÖSTER, H., QUAST, A. and REDEKER, G. Laminarization of transport aircraft wings – a German view, AIAA Paper 87-005, January 1987.
36. EPPLER, R. *Airfoil Program System 'PROFIL07' User's Guide*, Richard Eppler, Stuttgart, Germany, 2007.
37. DRELA, M. XFOIL: An analysis and design system for low Reynolds number airfoils, in: *Low Reynolds Number Aerodynamics*, MUELLER, T.J. (Ed), Lecture Notes in Engineering, **54**, Springer-Verlag, Berlin, Germany, 1989, pp 1–12.
38. DRELA, M. Design and optimization method for multi-element airfoils, AIAA Paper 93-0969, February 1993.
39. VAN INGEN, J.L. A suggested semi-empirical method for the calculation of the boundary-layer transition region, Rep VTH-74, Dep. Aeronaut. Eng, Technol. Univ. Delft, Netherlands, 1956.
40. SMITH, A.M.O. and GAMBERONI, N. Transition, Pressure Gradient and Stability Theory, Rep. No. ES 26388, Douglas Aircraft Co, 1956.
41. VAN INGEN, J.L., BOERMANS, L.M.M. and BLOM, J.J.H. Low-speed airfoil section research at Delft University of Technology, ICAS-80-10.1, Munich, Germany, October 1980.
42. BROPHY, C.M. Turbulence Management and Flow Qualification of The Pennsylvania State University Low Turbulence, Low Speed, Closed Circuit Wind Tunnel, MS Thesis, Pennsylvania State University, Pennsylvania, USA, 1993.
43. VON DOENHOFF, A.E. and ABBOTT, F.T. JR The Langley two-dimensional low-turbulence pressure tunnel, NACA TN 1283, 1947.
44. MCGHEE, R.J., BEASLEY, W.D. and FOSTER, J.M. Recent modifications and calibration of the Langley Low-Turbulence Pressure Tunnel, NASA TP-2328, 1984.
45. THIES, W. *Eppler-Profile* (*Eppler Airfoils*), Tenth ed., Modell-Technik-Berater 1/2, Verlag für Technik u. Handwerk, GmbH, Baden-Baden, Germany, 1986.
46. SOMERS, D.M. and MAUGHMER, M.D. Experimental results for the E 387 airfoil at low Reynolds numbers in The Pennsylvania State University Low-Speed, Low-Turbulence Wind Tunnel, US Army RDECOM TR 07-D-32, 2007. (Available from DTIC.)
47. MCGHEE, R.J., WALKER, B.S. and MILLARD, B.F. Experimental results for the Eppler 387 airfoil at low Reynolds numbers in the Langley Low-Turbulence Pressure Tunnel, NASA TM-4062, 1988.
48. SOMERS, D.M. Design and experimental results for the S805 airfoil, NREL/SR-440-6917, January 1997.
49. MEDINA, R. Validation of The Pennsylvania State University Low-Speed, Low-Turbulence Wind Tunnel Using Measurements of the S805 Airfoil, MS Thesis, Pennsylvania State University, Pennsylvania, USA, 1994.
50. SOMERS, D.M. Design and experimental results for the S809 airfoil, NREL/SR-440-6918, January 1997.
51. SOMERS, D.M. Design and experimental results for the S825 airfoil, NREL/SR-500-36346, January 2005.
52. WORTMANN, F.X. Experimental investigations on new laminar profiles for gliders and helicopters, TIL/T.4906, British Ministry Aviation, March 1960. (Translated from *Z Flugwissenschaften*, August 1957, **5**, (8), pp 228–243.)
53. EPPLER, R. and SOMERS, D.M. Airfoil design for Reynolds numbers between 50,000 and 500,000, in: *Proceedings of the Conference on Low Reynolds Number Airfoil Aerodynamics*, UNDAS-CP-77B123, University of Notre Dame, Indiana, USA, June 1985, pp 1–14.
54. HAMA, F.R. An efficient tripping device, *J Aeronaut Sci*, March 1957, **24**, (3), pp 236–237.
55. VAN INGEN, J.L. AND BOERMANS, L.M.M. Research on laminar separation bubbles at Delft University of Technology in relation to low Reynolds number airfoil aerodynamics, in: *Proceedings of the Conference on Low Reynolds Number Airfoil Aerodynamics*, UNDASCP-77B123, University of Notre Dame, Indiana, USA, June 1985, pp 89–124.
56. EPPLER, R. Laminar airfoils for Reynolds numbers greater than 4 × 10^6, B-819-35, April 1969. (Available from NTIS as N69-28178; translated from *Ingenieur-Archiv*, 1969, **38**, (4/5), pp 232–240).
57. SOMERS, D.M. Effects of airfoil thickness and maximum lift coefficient on roughness sensitivity, NREL/SR-500-36336, January 2005.
58. MAUGHMER, M.D. and SOMERS, D.M. Figures of merit for airfoil/aircraft design integration, AIAA Paper 88-4416, September 1988.
59. SMITH, A.M.O. High-lift aerodynamics, AIAA Paper 74-939, August 1974.
60. PFENNINGER, W. Investigations on reductions of friction on wings, in particular by means of boundary layer suction, NACA TM 1181, 1947. (Translated from Mitteilungen aus dem Institut für Aerodynamik an der Eidgenössischen Technischen Hochschule Zürich, Nr. 13, 1946.)
61. SOMERS, D.M. Laminar-flow airfoil, US Patent 6,905,092 B2, June 2005.
62. SOMERS, D.M. and MAUGHMER, M.D. Design and experimental results for the S414 airfoil, U.S. Army RDECOM TR 10-D-112, 2010. (Available from DTIC.)
63. GÖRTLER, H. On the three-dimensional instability of laminar boundary layers on concave walls, NACA TM 1375, 1954.
64. MAUGHMER, M.D. and CODER, J.G. Comparisons of theoretical methods for predicting airfoil aerodynamic characteristics, US Army RDECOM TR 10-D-106, 2010. (Available from DTIC.)

https://doi.org/10.1017/S0001924000005546 Published online by Cambridge University Press